



HAL
open science

Protein-surface interactions at the nanoscale: Atomistic simulations with implicit solvent models

David Malaspina, Leonor Pérez-Fuentes, Carlos Drummond, Delfi Bastos-González, Jordi Faraudo

► To cite this version:

David Malaspina, Leonor Pérez-Fuentes, Carlos Drummond, Delfi Bastos-González, Jordi Faraudo. Protein-surface interactions at the nanoscale: Atomistic simulations with implicit solvent models. *Current Opinion in Colloid & Interface Science*, 2019, 41, pp.40-49. 10.1016/j.cocis.2018.11.005 . hal-01962389

HAL Id: hal-01962389

<https://hal.science/hal-01962389v1>

Submitted on 25 Nov 2020

HAL is a multi-disciplinary open access archive for the deposit and dissemination of scientific research documents, whether they are published or not. The documents may come from teaching and research institutions in France or abroad, or from public or private research centers.

L'archive ouverte pluridisciplinaire **HAL**, est destinée au dépôt et à la diffusion de documents scientifiques de niveau recherche, publiés ou non, émanant des établissements d'enseignement et de recherche français ou étrangers, des laboratoires publics ou privés.

Protein - surface interactions at the Nanoscale: atomistic simulations with implicit solvent models

David C. Malaspina^a, Leonor Pérez-Fuentes^b, Carlos Drummond^c, Delfi Bastos-González^b, Jordi Faraudo^{*a}

^a*Institut de Ciència de Materials de Barcelona (ICMAB-CSIC), Campus de la UAB, E-08173 Spain*

^b*Biocolloid and Fluid Physics Group, Department of Applied Physics, University of Granada, Av. Fuentenueva 2, E-18001 Granada (Spain)*

^c*CNRS, Centre de Recherche Paul Pascal (CRPP), UMR 5031, Pessac, France*

Abstract

A full molecular-level understanding of protein adsorption in important situations such as the formation of protein films at solid/liquid interfaces or the formation of a protein corona over inorganic nanoparticles is still lacking. All-atomic implicit solvent molecular dynamics (MD) simulations, which are successfully employed in many related protein studies (such as protein folding for example) are emerging also as a useful tool to investigate proteins at surfaces. Implicit solvent simulations replace the detailed description of the solvent by a continuum media and effective atom-atom interactions retaining the atomistic detail in the description of the system of interest. This allows the simulation of larger systems and longer time scales as compared with full MD simulations including explicit solvent. In this brief review, we present an overview of the current state of the application of this technique to the study of problems such as the interaction of proteins with solid surfaces and the structure of protein corona over inorganic nanoparticles. Limitations of the approach and future perspectives are also outlined.

Keywords: Molecular Dynamics, Implicit solvent models, Protein surface interaction, Protein corona

Email address: jfaraudo@icmab.es (Jordi Faraudo*)

1. Introduction

Protein adsorption at interfaces has been described several times as a "common but very complicated phenomenon" [1, 2]. Different factors which are difficult to quantify such as the softness and hydrophobic or hydrophilic character of the protein or surface polarity for example are thought to play a decisive role in the properties of adsorbed protein layers and in biomaterials design [3]. In the bionanotechnology field, protein adsorption also has a prominent role. Nanoparticles (NP) in contact with biological fluids, are rapidly covered by a protein corona which determines the interactions and the biological identity of the material [4]. In fact, tailoring the protein corona is an essential step in drug delivery applications of NPs [5, 6].

Our ability to predict the behaviour and properties of proteins is growing rapidly due to the substantial increase in our knowledge of protein structure with atomistic resolution. For example, the Protein Data Bank [7, 8] contains the atomic coordinates of about 1.4×10^5 structures (and growing, at a rate of 10^4 structures per year), resolved by methods such as X-ray or NMR. In principle, these structures can be used, in combination with theoretical methods, to predict the interactions of proteins with materials and tackle the open questions related to protein adsorption, protein films and protein corona from a rational design perspective. To this end, a suitable computational tool is of course needed. A fitting candidate as a tool for performing such theoretical investigation is Molecular Dynamics simulations (MD). Conceptually, the method is simple. It is based on the fact that at ordinary conditions (not under extreme temperatures or pressures), the motion of atoms of any molecular system can be computed implementing numerically the Newton laws of motion in a computer. The method of course needs an accurate description of the interaction forces between atoms (belonging to the same or different molecules), which can be done with good approximation using suitable, well-known force fields in many situations. The problem for the use of MD simulations for the study of protein-surface interactions is in the limitations of the method for dealing with large number of atoms and long time scales. For example, an atomistic model of a simple protein such as BSA has ≈ 9200 atoms (including hydrogen atoms). The protein corona of a 6 nm nanoparticle (NP) contains ≈ 10 BSA proteins[9], so the number of atoms required to model the proteins and the NP is $\approx 10^5$. The process of protein adsorption takes place always in water, so the addition of a water box large enough to have the proteins and NP in suspension in such

38 a hypothetical simulation will increase the number of atoms by an order of
39 magnitude, making the simulation impossible. An additional limitation is
40 related to time scales. MD simulations in explicit solvent are typically lim-
41 ited to time scales of the order of $\approx 10^2$ ns, which are too short to describe
42 important processes such as protein diffusion or rearrangement at surfaces.
43 For these reasons, the modelling of protein-surface interaction has been al-
44 most exclusively based on simplified models, which take into account the
45 protein structure from a coarse-grained perspective. However, the develop-
46 ment of implicit solvent force fields has allowed simulations of many complex
47 systems involving proteins with full atomistic detail. In these models, water
48 molecules are not included explicitly and the interaction of atoms from the
49 protein are modified from classical force fields to include the effect of wa-
50 ter in an implicit way [10, 11, 12, 13]. In this way, it is possible to reduce
51 the number of atoms in the MD simulation to an affordable amount, with a
52 concomitant reduction in the number of atom-atom interactions to be calcu-
53 lated in the simulation. It has to be noted that in implicit solvent all-atomic
54 models, atom-atom interactions are more computationally expensive to cal-
55 culate than in explicit solvent models [12, 13], but the overall balance is that
56 simulations with implicit solvent models are (in general) substantially faster
57 than explicit solvent simulations. Using these models, it has been possible
58 to investigate with atomistic detail many interesting processes such as the
59 structure of protein corona of a NP [14, 9] or how proteins adsorbed onto
60 a surface respond to a pH change [15], among others, as we will see. Our
61 objective in this article will be to summarize these developments. Of course,
62 as any approach to a difficult problem, these simulations have their own
63 difficulties and limitations, which we will also discuss.

64 The paper is organized as follows. In section 2, we will briefly discuss
65 the conceptual aspects of Implicit solvent molecular dynamics simulations.
66 In Section 3 we will discuss some basic results obtained from implicit solvent
67 MD simulations of adsorption of a single protein onto a surface. In Section
68 4, we will discuss implicit solvent MD simulations involving the interaction
69 between several proteins at a surface, such as protein films and protein corona
70 of NPs. Finally, we will end up with Conclusions and Perspectives.

71 **2. Implicit solvent models for all-atomic Molecular Dynamics sim-** 72 **ulations of proteins**

73 In implicit solvent models, the solvent is replaced by a continuum di-
74 electric medium and the expressions employed to compute the interactions
75 between atoms are modified (from those employed with explicit water) to
76 include the solvent in an effective way [10, 11, 13]. The first implicit solvent
77 force field now known as Generalized Born Implicit Solvent model (GBIS,
78 also sometimes abbreviated as GBSA to emphasize the inclusion of the ef-
79 fects due to the solvent accessible surface) was originally proposed in the 90s
80 [10] to describe the interaction energy between molecules in solution for use
81 in molecular dynamics simulations without the need to describe explicitly the
82 solvent molecules. The main concept in the GBIS force field is to combine the
83 concepts of classical force fields for explicit solvent MD simulations with the
84 basic concepts of the Born theory of molecular solvation and the basic theory
85 of the hydrophobic effect. In its original formulation [10], MD simulations
86 employing the GBIS force field described with a very good approximation
87 the solvation free energy of a wide range of small molecules, from inorganic
88 ions to organic molecules. However, the theory produced inaccurate results
89 in the case of molecules with large interior regions with many atoms buried
90 inside, as in the case of proteins [16]. Over the years, refinements in the cal-
91 culation of the dielectric screening [17] and electrostatics near the surfaces of
92 the atoms [11] provided the necessary improvements and good results were
93 obtained when used with MD of proteins. The accuracy of the current ver-
94 sions of the GBIS forcefield for MD simulations of biomolecules is discussed
95 in many reviews (see for example [18, 19]). Nowadays, implementations of
96 GBIS force-fields for implicit solvent MD simulations are available in stan-
97 dard MD codes such as AMBER [11], NAMD [12, 13] or GROMACS [20].

98 The GBIS implicit solvent force field, as implemented in the MD codes
99 mentioned above, describe the atoms with the same atomic partial charges
100 and Lennard-Jones atomic parameters as employed in the explicit solvent
101 force field for the calculation of electrostatic and Van der Waals interac-
102 tions. However, two substantial modifications are made in the energy and
103 force equations of the force field. The first modification is that electrostatic
104 interactions are calculated using a modified expression (instead of a direct
105 Coulomb’s law) which takes into account the degree of exposure of each
106 atom to the solvent [10, 11]. And the second modification is that hydropho-
107 bic interactions are included as an additional term in the force field which

108 is proportional to the exposed hydrophobic surface and an effective surface
109 tension of the molecule-solvent interface [10, 13].

110 The modified expression for the electrostatic interaction has a more com-
111 plex spatial dependence than Coulomb’s law, and it contains as a fundamen-
112 tal quantity determining the length scale of the interactions, the so-called
113 Born radii. Each atom in a molecule is represented by an sphere filled uni-
114 formly with material of dielectric constant $\epsilon_r=1$ [11]. The exterior of the
115 atom is filled with a continuum medium with an effective dielectric constant
116 of the solvent which also depends on the implicit ion concentration [13]. The
117 size of the atom is given by the Born radius which describes the exposure
118 of a given atom to the solvent (thus determining the degree of screening of
119 electrostatic interaction by the solvent). The Born radius depends on the dis-
120 tance to neighbouring atoms. For an isolated atom, its Born radius is equal
121 to its van der Waals radius [21], while for a deeply buried atom, its Born
122 radius is much larger than its Van der Waals radius. Depending on the spe-
123 cific implementation of the GBIS force field, the Born radius is calculated by
124 the Onufriev-Bashford-Case (OBC) method [11] or by the Hawkins-Cramer-
125 Truhlar method [17].

126 We recall here that the generalized Born implicit solvent GBIS model de-
127 scribed above gives an accurate description of the polar contribution to the
128 energy of solvation. The second modification of the force field for implicit sol-
129 vent accounts for the nonpolar (i.e. hydrophobic) contribution to the energy
130 of solvation. As we said, the model assumes that the nonpolar, hydrophobic
131 solvation energy is proportional to the exposed hydrophobic surface, with a
132 surface tension ≈ 0.005 kcal/mol \AA^2 [13] which is a typical value for hydro-
133 carbons in water. This is calculated by computing the surface exposed by
134 each atom weighted by an atom-type weight.

135 Using an implicit solvent force field, one reduces greatly the number of
136 atoms in the simulation and more importantly the number of atom pair inter-
137 actions to be computed. But the price to pay is an increased computational
138 cost of the calculations. The increased computational time has two sources.
139 First, in the GBIS model, it is not possible to use the Particle Mesh Ewald
140 (PME) method to speed up electrostatic calculations [12, 13], as it is usually
141 done with Coulomb interactions in explicit solvent MD simulations. The only
142 option in GBIS force fields is to compute long-range screened electrostatics
143 with a large cut off. The second source of increased computational cost
144 is related to the complexity of the GBIS equations (which require also the
145 calculation of the Born radius which depends on the distribution of atoms).

146 Typical estimations suggest that electrostatic GBIS calculations are typically
147 7 times more expensive than PME electrostatic calculations [13].

148 The actual source of speed up of implicit solvent MD simulations is due
149 to two factors: a) the absence of viscosity (which induces faster speed in
150 relaxation processes) and b) absence of slow processes involving explicit water
151 molecules. Therefore, the comparison between the actual gain in implicit
152 solvent MD depends on the amount of water required in the simulation box
153 to perform the explicit solvent simulation of the same problem. This balance
154 is nicely illustrated by the calculations reported in Ref [22]. For example,
155 an implicit solvent MD simulation of a 25,100-atom model of a nucleosome
156 is nominally 1.6 times slower than the explicit-solvent PME simulation with
157 a small water solvent box extending 1 nm from the solute, whereas it is 1.6
158 times faster compared to a PME simulation in a larger 3.6 nm water solvent
159 box.

160 Another important point, in order to compare implicit solvent and ex-
161 plicit solvent MD simulations is that nominal simulation time (this is, the
162 time step in real units multiplied by the number of steps) has different mean-
163 ings. In an explicit solvent MD simulation, the nominal simulation time is
164 expected to correspond to the clock time elapsed in the real system in an
165 equivalent experimental situation. But in the case of implicit solvent models,
166 the absence of explicit water molecules and the absence of viscosity implies
167 that the exploration of the configuration space takes place at a higher speed
168 than in a real situation. In other words, for each ns of simulation, a protein
169 will explore more possible configurations in an implicit solvent MD simula-
170 tion than in an explicit solvent MD simulation. Therefore, the quantification
171 of the speed up obtained in implicit solvent models is not a trivial task. This
172 question has been investigated in detail in Ref [22] by comparing the speed
173 of five different conformational changes in implicit solvent and explicit sol-
174 vent MD simulations (a dihedral angle flip, nucleosome histone tail collapse,
175 DNA unwrapping from the nucleosome histone tail collapse, DNA unwrap-
176 ping from the nucleosome histone core and miniprotein folding). The authors
177 compare not only the differences in nominal simulation times for explicit and
178 implicit water but also estimate the time that will correspond to a explicit
179 water simulation to explore the configurations obtained in the trajectories of
180 the implicit model MD simulations. Taking into account all these factors,
181 the speed up of the conformational change in implicit solvent was shown to
182 be strongly depended on the particular problem. In the case of a dihedral
183 angle flip, the speed up is only by a factor of 1.6 whereas that in the case of

184 miniprotein folding the speed up is by a factor of ≈ 54 .

185 Concerning the accuracy of implicit solvent models, comparison with ex-
186 plicit solvent models [11, 12, 13, 22] reveals that implicit solvent MD simula-
187 tions predict correctly protein configuration in bulk conditions, as compared
188 with explicit solvent simulations and experimental data. Now the question is
189 the performance of the implicit solvent models in the case of the interaction
190 of proteins with surfaces.

191 **3. MD simulations of the adsorption of a single protein**

192 Once the validity of the implicit solvent MD simulations of proteins has
193 been established (see Section 2), the next step is to consider the adsorption
194 of a single protein onto a surface. Albeit simple, there are many interest-
195 ing questions that have been studied from such simulations, as illustrated
196 in Figure 1. Some of these questions are the identification of the specific
197 amino acids involved in the adsorption of a given protein at a given surface
198 (and thus the driving force for adsorption), structural changes of proteins
199 after adsorption, the effect of changing conditions (such as pH) after protein
200 adsorption or the effect of curvature in adsorption (adsorption onto a planar
201 surface compared with adsorption onto small nanoparticles).

202 We will discuss now some representative results related to these ques-
203 tions, by comparing the results obtained for different proteins and different
204 substrates. In Figure 1, we summarize the results obtained in the case of
205 four different systems: (a) the adsorption of β -Lactoglobulin onto a planar
206 metal surface [23], (b) the adsorption of β -casein onto a generic model of
207 a planar hydrophobic surface, (c) the adsorption of ubiquitin onto a 10 nm
208 diameter Ag nanoparticle and (d) the adsorption of a BSA protein onto a 6
209 nm diameter nanoparticle.

210 In all these cases, the implicit solvent simulations allowed to identify
211 the specific amino acids or the specific protein domain involved in adsorp-
212 tion, as shown in Figure 1. One interesting result obtained in some of these
213 simulations is that the residues involved in protein adsorption -for a given
214 protein- are essentially the same in different situations (such as for charged
215 or neutral surfaces or at different pH). For example, in the case of bovine
216 β -Lactoglobulin [23] adsorbed onto a gold surface, it was found that the
217 residues involved in the adsorption were the same for a neutral surface or for
218 surfaces with different values of positive charge. The protein residues adsorb-
219 ing at the neutral Au surface are the hydrophilic Thr 125, Thr 18, Lys 100

220 and Gln 13 residues and the Pro 50 hydrophobic residue (see Figure 1a). In
221 the simulations, the effect of charging the surface with positive charge den-
222 sity was also investigated. When charging the surface, some residues from
223 125 to 135 (which are close to the surface in the neutral surface case) also
224 change its charge, leading to stronger adsorption by attractive electrostatic
225 residuesurface interactions.

226 Analogous results were obtained in [15] for adsorption of β -casein onto
227 model hydrophobic surfaces of different charges (Figure 1b). At neutral pH,
228 the negatively charged protein (with a charge of $-6e$) adsorbs onto a neutral
229 hydrophobic surface by contact with several, mostly hydrophobic residues
230 but also by some polar residues situated near these hydrophobic ones. The
231 residues involved in the contact between the protein and the neutral surface
232 were six hydrophobic aminoacids (Pro 76, 78, 194, 196, 201 and Phe 205),
233 and three polar aminoacids (Tyr 75, Val 193 and Ile 202), all indicated in
234 Figure 1b). No significant change in the adsorption of the protein (same
235 adsorbed residues and same area of contact) was observed when changing
236 the charge of the surface from neutral to negative (-0.62 e/nm^2), in spite of
237 the electrostatic repulsion (recall that both the surface and the protein were
238 negatively charged). Finally, the charge of the adsorbed protein was changed
239 from $-6e$ to $+8e$, corresponding to a pH change from 7 to 4 (the charge of
240 the surface was maintained unchanged at -0.62 e/nm^2). In this case, the
241 adsorbed protein increases the contact with the surface, by adsorbing not
242 only with the same residues as in the case of neutral pH but also with other
243 protonated, positively charged residues located near the previously adsorbed
244 domain.

245 In addition to these studies over planar surfaces, there are also a few
246 simulations [9, 14] that study similar questions in the case of adsorption of
247 proteins over NPs. These studies are more difficult than simulations over a
248 planar surface (because they involve the simulation of the full NP) and are
249 typically restricted to small NPs, with sizes of 5-10 nm.

250 In Ref. [14], the authors studied the adsorption of ubiquitin over a 10 nm
251 Ag NP. They found that the protein adsorbs by binding of the Asp 18 residue
252 to the NP (see Figure 1c) and also to some extent with an interaction of the
253 Gln 8 residue with the NP. No significant change in the secondary structure
254 of the protein was found due to adsorption. These simulation results are
255 in agreement with NMR studies [24] which found that the binding domain
256 of human ubiquitin to Ag NP was located in the residues Gln 2-Ile 3 and
257 Leu 15-Asp 18 . Concerning the kinetics of adsorption, they obtained that

258 protein re-orientation was the rate-limiting step in protein adsorption.

259 In Ref. [9], the authors studied experimentally and by MD implicit solvent
260 simulations the adsorption of BSA onto a 6 nm iron oxide NP covered by
261 citrate. The simulations show that as the protein contacts the NP, the BSA
262 protein changes its conformation and the protein domain in contact with the
263 NP partially spreads over the surface of the NP (see Figure 1d). In fact,
264 the surface of the protein increased from 325 nm² in solution to 345 nm²
265 at the NP surface. The change in the secondary structure of the protein
266 was small; the α -helix content changed from 72% in solution to 66% for
267 a BSA adsorbed onto a NP. However, a few residues changed significantly
268 its environment. It was particularly interesting the case of the Trp213 and
269 Trp134 residues which contribute to the UV-vis spectra of the BSA protein.
270 Simulations also indicate a change of their environment from being buried
271 into the protein to a more solvent exposed location, a result in agreement
272 with UV-vis spectroscopy measurements [9].

273 All the simulation results discussed so far of MD simulations with implicit
274 solvent indicate a small change in the conformation of a protein after adsorp-
275 tion, with the changes localized at a few particular residues. Probably the
276 most significant exception is the case of adsorption of proteins at carbon sur-
277 faces (graphite or graphene) in which several works using implicit solvent MD
278 simulations report substantial unfolding of proteins or protein fragments over
279 these carbon surfaces. Examples include unfolding of albumin and fibronectin
280 fragments after adsorption onto graphite and carbon nanotubes [25], unfold-
281 ing of lysozyme on graphite [26] and unfolding of a BMP-2 protein onto
282 graphite [27]. Interestingly, the results for unfolding of BMP-2 protein onto
283 graphite[28] were further confirmed by MD simulations in explicit solvent
284 using accelerated MD simulations. Other explicit solvent MD simulations
285 of proteins and peptides onto carbon surfaces indicate similar conclusions.
286 Explicit solvent MD simulations of two "de novo" designed α -helical pep-
287 tides [29] show that they unfold and assemble into an amorphous dimer at
288 a graphene surface, in agreement with circular dichroism spectroscopy and
289 scanning tunneling microscopy measurements. It seems that the specific role
290 of the carbon surface is important in these results. For example, extensive
291 explicit solvent simulations of lysozyme adsorption/desorption on polymeric
292 hydrophobic surfaces [30, 31] only show small secondary structure changes
293 in particular residues (typically those located near the adsorption region),
294 but they do not show unfolding of the protein. Interestingly, in these works
295 it was found that there is an energy barrier for adsorption mainly arising

296 from protein and surface hydration in the first hydration shell. The protein
297 cannot be adsorbed even though the substrate surface exhibits attraction,
298 whenever the proteinsurface interaction energy is not large enough to over-
299 come the barrier of breaking the hydration shells, which is strongly residue
300 and surface dependent.

301 The question of the specific role of carbon surfaces in protein unfolding
302 and the validity of its modelling by using implicit solvent MD simulations
303 was analysed in detail in Ref. [32]. First, the authors repeated and ex-
304 tended previous studies [33] which reported unfolding of BSA after adsorp-
305 tion onto graphene. They found large unfolding of BSA upon adsorption onto
306 a graphene surface, with an α -helix content of only 35% after free adsorption
307 onto graphene. The authors also reported extensive all-atomic MD simu-
308 lations of BSA adsorption onto graphene with explicit solvent and in this
309 case the α -helix content was about 60% after free adsorption. Therefore,
310 in this case the unfolding of BSA was observed only in the case of implicit
311 solvent MD simulations. This discrepancy probably indicates that the em-
312 ployed force field for carbon surfaces greatly exaggerates the strength of the
313 interaction of BSA with graphene, inducing a BSA unfolding as a simulation
314 artefact. We think that better, thoroughly validated force fields for implicit
315 solvent simulations of carbon surfaces are needed for implicit solvent sim-
316 ulations of protein adsorption. As a general consequence, we can say that
317 more attention has to be paid to implicit solvent models of surfaces for use
318 in implicit solvent simulations involving biomolecular adsorption.

319 Another interesting question to discuss, in light of simulation results, is
320 the reversibility or irreversibility of protein adsorption. In all the simulations
321 discussed so far, only adsorption (with no desorption) was reported, indicat-
322 ing that protein adsorption is essentially irreversible at the time scales probed
323 by atomistic MD simulations. This question has been discussed in a recent
324 all-atomic MD study (with explicit solvent) of the energy landscape for BSA
325 adsorption onto silica [34]. The results indicate that the time scales for pro-
326 tein desorption are of orders of hours in this case, whereas time scales for
327 protein diffusion are in the 100 ns range. Therefore, protein desorption is
328 far beyond the scales accessible to MD (even with implicit solvent models)
329 whereas protein diffusion should be observable, if present, by all-atomic MD
330 simulations.

331 **4. MD Simulations of adsorption of many proteins: protein films**
332 **and protein corona**

333 Most of the simulation results published in the literature correspond to
334 the situation considered in Section 3, this is, the interaction of a single protein
335 with a planar surface or a nanoparticle, which correspond to studies of the
336 protein-surface interaction.

337 Of course, as the coverage of adsorbed protein increases, protein-protein
338 interactions became more and more important, but these situations are com-
339 putationally expensive because they require the consideration of many pro-
340 teins at the surface. The cost of the simulations increases not only because
341 the number of atoms in the simulation increases but also because the dy-
342 namics of the problem itself is much slower. This makes the simulation of
343 high coverages prohibitively expensive in many cases. For this reason, only
344 recently simulations considered atomistic simulations of protein films or pro-
345 tein corona in which protein-protein interactions are essential. In spite of
346 these difficulties, a few of the studies discussed in the previous section con-
347 sider not only the case of a single protein adsorption but also the formation
348 of an adsorbed protein layer with atomistic detail, which we will now discuss.

349 In addition to the study of single β -casein protein adsorption (discussed
350 in Section 3, see Figure 1b), this work also considered simulations with two
351 and three adsorbed proteins onto a surface of 45.5 nm^2 . These simulations
352 with two and three proteins correspond to a mass coverage of 1.74 mg/m^2 ,
353 and 2.6 mg/m^2 which are about 47% and 70% of the maximum experimental
354 coverage for a β -casein monolayer [15]. Comparing the simulation results at
355 the different coverages (see Figure 2a), it was observed that the thickness
356 of the film decreases from $\approx 4 \text{ nm}$ at the lowest coverage to $\approx 3 \text{ nm}$ at the
357 highest coverage, indicating that at higher coverages the proteins tend to
358 be adsorbed in a more compact configuration. As shown in the snapshot in
359 Figure 2b, the adsorbed proteins are in contact, forming a compact structure.
360 Hence, the results indicate a substantial protein-protein attraction in spite
361 of the electrostatic repulsion between proteins (each protein has a charge of
362 $-8e$ in the simulation, corresponding to $\text{pH}=7$).

363 The case of the maximum possible coverage was considered in the case of
364 the formation of a BSA protein corona onto a 6 nm diameter nanoparticle
365 studied in Ref. [9] (see Figure 1c). In that case, the simulations were em-
366 ployed to determine the number of proteins in the corona, their organization
367 and to identify possible secondary structure differences between proteins in

368 the corona or free proteins. It should be noted also that the BSA protein is
369 commonly employed in experiments as a cheaper alternative to experimenta-
370 tion with the human serum albumina (HSA) protein, which is more relevant
371 for biomedical applications. For this reason, we have also repeated the anal-
372 ysis in [9] using HSA instead of BSA [35] and we have also considered two
373 different particle sizes (6 nm and 3 nm of diameter). Starting from the sim-
374 ulation with a single adsorbed protein, the simulations of the protein corona
375 were done by systematically adding more proteins in solution to a previous
376 simulation (see [9]) with a smaller number of proteins and performing long
377 simulation runs in order to allow for structural relaxations and adsorption of
378 additional proteins [9]. It should be noted that the total number of atoms
379 in these simulations with many proteins is $\approx 10^5$ atoms (for a 10 protein
380 simulation) while the same system in explicit solvent would have more than
381 1 million of atoms in the simulation box. The simulations indicate that the
382 maximum number of BSA or HSA proteins that can be accommodated onto
383 the 6 nm NP is of 10 proteins (see Figure 2b), a result which is in agree-
384 ment with experiments [9] (in which the number of BSA at the corona was
385 estimated from the change in size of the particle before and after protein
386 corona formation). It is also interesting to recall that the maximum number
387 of proteins considered in the simulations was 12 and that in these simula-
388 tions with excess protein, 2 of the proteins remain in bulk without adsorbing
389 and without interacting significantly with the layer of adsorbed proteins [9].
390 This result also suggests that these proteins form only a monolayer over the
391 NP, since a soft corona (a second layer of protein adsorbed onto the protein
392 corona) was not observed in our simulations.

393 The size of the NP has a deep impact in the size and organization of the
394 protein corona, as can be seen in Figure 2c. In the case of a 3 nm NP, we
395 obtain a protein corona of only 3 HSA proteins which are clearly separated
396 (i.e., they are not in contact) due to the curvature of the surface. This has to
397 be compared with the compact structure made by the 10 proteins adsorbed
398 onto a 6 nm NP (also note here that a decrease of the surface by a factor of
399 4 involved a decrease in the number of proteins by a factor of 3.3).

400 In Figure 2, we also show structural details that can be obtain from data
401 analysis of the simulations. In figure 2d, we compare the α -carbon radial
402 density data from Ref. [9] for BSA or HSA protein corona [35] respectively
403 of a 6 nm NP. The results were very similar in both cases. There is a high
404 density peak at the NP surface and a constant density region (the compact
405 corona) that extends up to a distance of 6.5 nm of the centre of the NP. This

406 corresponds to a diameter of the NP+protein corona entity of about 13 nm,
407 in agreement with DLS measurements with BSA [9].

408 As we discussed before, implicit solvent models can provide accurate rep-
409 resentation of protein secondary structure, so we can discuss the secondary
410 structure of the proteins in the protein corona. Figure 2c shows the α -helix
411 content for each of the HSA or BSA proteins adsorbed on the protein corona,
412 compared with a protein in bulk solution. The results show that the changes
413 in secondary structure are small in all cases, but there is also a tendency
414 indicating that these changes are smaller for the last adsorbed proteins. The
415 explanation for this effect is that at low coverages, there is more space avail-
416 able for the spreading of the protein over the surface (recall here previous
417 section and Figure 1b). On the contrary, near saturation, the last adsorbed
418 protein has a small surface available for adsorption and a small contact with
419 the NP, without possibility of spreading over the surface.

420 5. Conclusions and outlook

421 Implicit solvent models for protein simulation are an interesting alterna-
422 tive for simulations of proteins retaining all-atomic details with affordable
423 resources. Their use in the study of problems involving protein adsorption
424 onto surfaces, such as protein films or the protein corona of NPs is a young
425 and promising approach that has delivered several interesting insights but
426 still has drawbacks that need to be tackled. We can summarize the ac-
427 complishments and shortcomings of MD atomistic simulations of proteins at
428 surfaces using implicit solvent GB models as follows:

- 429 • The method can be used for atomistic simulation of protein films over
430 planar surfaces under different conditions (e.g. different pH) even in
431 the case of protein and surface charged with charges of the same sign.
- 432 • The method can be used for atomistic simulation of protein corona
433 over small NPs (≤ 10 nm). Predictions of the size of protein corona are
434 in agreement with experimental results. The method is currently the
435 only feasible option to study, with atomistic detail, the structure of a
436 protein corona and its interactions with their environment.
- 437 • Predictions of secondary structure changes after adsorption are in gen-
438 eral in agreement with experimental data.

- 439 • The model of the surface must be consistent with the implicit solvent
440 model employed for the description of the protein. This is in gen-
441 eral a nontrivial question, so some kind of validation of the results
442 (by comparing with reference simulations with explicit solvent or with
443 experimental results) is advisable.
- 444 • The role of ions is considered in a implicit way, at a Poisson-Boltzmann
445 level of description. This is clearly not enough for describing the com-
446 plex specific effects of ions with proteins, which are know to play a
447 substantial role in protein films [36].
- 448 • Charge regulation effects taking place during protein adsorption (pro-
449 tonation or deprotonation of charged groups at the surface and/or pro-
450 tonation or deprotonation of protein residues near the surface) are im-
451 portant, but not considered in MD simulations.

452 As we have discussed in this review, the direction of the field in the last years
453 has been clearly focused on the implementation of the method in the software
454 usually employed in MD simulations and to speed up the implementations
455 of the method (by adding features such as the use of GPU). We are sure
456 that these implementations of the method will fuel exciting new uses of the
457 method to study more complex problems. But before more applications of
458 greater complexity can be considered, it will be of a great interest to advance
459 and improve the theory. We think that, in view of the points listed above, the
460 most pressing questions to be tackled are the development of more accurate
461 implicit solvent models for nanostructured surfaces of interest and also the
462 development of consistent models for the explicit inclusion of ions (and their
463 specific effects) and the inclusion of charge regulation in implicit solvent MD
464 simulations.

465 **Acknowledgements**

466 We acknowledge financial support from the Spanish Government grants
467 MAT2015-64442-R and SEV-2015-0496 and from the Junta de Andalucia
468 Grant CTS-6270. D.C.M. is supported by the European Unions Horizon 2020
469 research and innovation programme under Marie Sklodowska-Curie grant
470 agreement No 6655919.

471 **References**

- 472 [1] K. Nakanishi, T. Sakiyama, K. Imamura, On the adsorption of proteins
473 on solid surfaces, a common but very complicated phenomenon, *Journal*
474 *of Bioscience and Bioengineering* 91 (2001) 233–244.
- 475 [2] M. Rabe, D. Verdes, S. Seeger, Understanding protein adsorption phe-
476 nomena at solid surfaces, *Advances in Colloid and Interface Science* 162
477 (2011) 87–106.
- 478 [3] M. M. Ouberaï, K. Xu, M. E. Welland, Effect of the interplay between
479 protein and surface on the properties of adsorbed protein layers, *Bio-*
480 *materials* 35 (2014) 6157–6163.
- 481 [4] M. P. Monopoli, C. Åberg, A. Salvati, K. A. Dawson, Biomolecular
482 coronas provide the biological identity of nanosized materials, *Nature*
483 *Nanotechnology* 7 (2012) 779+.
- 484 [5] J. Mariam, S. Sivakami, P. M. Dongre, Albumin corona on nanoparticles
485 a strategic approach in drug delivery, *Drug Delivery* (2015) 1–9.
- 486 [6] V. H. Nguyen, B.-J. Lee, Protein corona: a new approach for
487 nanomedicine design, *International Journal of Nanomedicine Volume*
488 *12* (2017) 3137–3151.
- 489 [7] H. Berman, K. Henrick, H. Nakamura, Announcing the worldwide pro-
490 tein data bank, *Nature Structural Biology* 10 (2003) 980+.
- 491 [8] H. Berman, K. Henrick, H. Nakamura, J. L. Markley, The worldwide
492 protein data bank (wwPDB): ensuring a single, uniform archive of PDB
493 data, *Nucleic Acids Research* 35 (2007) D301–D303.
- 494 [9] S. Yu, A. Perálvarez-Marín, C. Minelli, J. Faraudo, A. Roig, A. Laro-
495 maine, Albumin-coated SPIONs: an experimental and theoretical eval-
496 uation of protein conformation, binding affinity and competition with
497 serum proteins, *Nanoscale* 8 (2016) 14393–14405.
- 498 [10] W. C. Still, A. Tempczyk, R. C. Hawley, T. Hendrickson, Semianalytical
499 treatment of solvation for molecular mechanics and dynamics, *Journal*
500 *of the American Chemical Society* 112 (1990) 6127–6129.

- 501 [11] A. Onufriev, D. Bashford, D. A. Case, Exploring protein native states
502 and large-scale conformational changes with a modified generalized born
503 model, *Proteins: Structure, Function, and Bioinformatics* 55 (2004)
504 383–394.
- 505 [12] D. E. Tanner, K.-Y. Chan, J. C. Phillips, K. Schulten, Parallel general-
506 ized born implicit solvent calculations with NAMD, *Journal of Chemical*
507 *Theory and Computation* 7 (2011) 3635–3642.
- 508 [13] D. E. Tanner, J. C. Phillips, K. Schulten, GPU/CPU algorithm for
509 generalized Born/Solvent-accessible surface area implicit solvent calcu-
510 lations, *J. Chem. Theory Comput.* 8 (2012) 2521–2530.
- 511 [14] F. Ding, S. Radic, R. Chen, P. Chen, N. K. Geitner, J. M. Brown,
512 P. C. Ke, Direct observation of a single nanoparticleubiquitin corona
513 formation, *Nanoscale* 5 (2013) 9162+.
- 514 [15] L. Pérez-Fuentes, C. Drummond, J. Faraudo, D. Bastos-González, Ad-
515 sorption of milk proteins (beta-casein and beta-lactoglobulin) and BSA
516 onto hydrophobic surfaces, *Materials* 10 (2017) 893+.
- 517 [16] J. Srinivasan, M. W. Trevathan, P. Beroza, D. A. Case, Application of a
518 pairwise generalized born model to proteins and nucleic acids: inclusion
519 of salt effects, *Theoretical Chemistry Accounts: Theory, Computation,*
520 *and Modeling (Theoretica Chimica Acta)* 101 (1999) 426–434.
- 521 [17] G. D. Hawkins, C. J. Cramer, D. G. Truhlar, Parametrized models
522 of aqueous free energies of solvation based on pairwise descreening of
523 solute atomic charges from a dielectric medium, *The Journal of Physical*
524 *Chemistry* 100 (1996) 19824–19839.
- 525 [18] J. Chen, C. L. Brooks, J. Khandogin, Recent advances in implicit
526 solvent-based methods for biomolecular simulations, *Current Opinion*
527 *in Structural Biology* 18 (2008) 140–148.
- 528 [19] J. Kleinjung, F. Fraternali, Design and application of implicit solvent
529 models in biomolecular simulations, *Current Opinion in Structural Bi-*
530 *ology* 25 (2014) 126–134.
- 531 [20] P. Bjelkmar, P. Larsson, M. A. Cuendet, B. Hess, E. Lindahl, Implemen-
532 tation of the CHARMM force field in GROMACS: Analysis of protein

- 533 stability effects from correction maps, virtual interaction sites, and wa-
534 ter models, *Journal of Chemical Theory and Computation* 6 (2010)
535 459–466.
- 536 [21] A. Bondi, van der waals volumes and radii, *The Journal of Physical*
537 *Chemistry* 68 (1964) 441–451.
- 538 [22] R. Anandakrishnan, A. Drozdetski, R. C. Walker, A. V. Onufriev,
539 Speed of conformational change: Comparing explicit and implicit sol-
540 vent molecular dynamics simulations, *Biophysical Journal* 108 (2015)
541 1153–1164.
- 542 [23] T. Hagiwara, T. Sakiyama, H. Watanabe, Molecular simulation of
543 bovine beta-Lactoglobulin adsorbed onto a positively charged solid sur-
544 face, *Langmuir* 25 (2009) 226–234.
- 545 [24] L. Calzolari, F. Franchini, D. Gilliland, F. Rossi, ProteinNanoparticle
546 interaction: Identification of the UbiquitinGold nanoparticle interaction
547 site, *Nano Letters* 10 (2010) 3101–3105.
- 548 [25] G. Raffaini, F. Ganazzoli, Understanding the performance of bioma-
549 terials through molecular modeling: Crossing the bridge between their
550 intrinsic properties and the surface adsorption of proteins, *Macromolec-
551 ular Bioscience* 7 (2007) 552–566.
- 552 [26] G. Raffaini, F. Ganazzoli, Protein adsorption on a hydrophobic surface:
553 A molecular dynamics study of lysozyme on graphite, *Langmuir* 26
554 (2010) 5679–5689.
- 555 [27] C. Mücksch, H. M. Urbassek, Adsorption of BMP-2 on a hydrophobic
556 graphite surface: A molecular dynamics study, *Chemical Physics Letters*
557 510 (2011) 252–256.
- 558 [28] C. Mücksch, H. M. Urbassek, Enhancing protein adsorption simulations
559 by using accelerated molecular dynamics, *PLoS ONE* 8 (2013) e64883+.
- 560 [29] L. Ou, Y. Luo, G. Wei, Atomic-Level study of adsorption, conforma-
561 tional change, and dimerization of an α -Helical peptide at graphene sur-
562 face, *The Journal of Physical Chemistry B* 115 (2011) 9813–9822.

- 563 [30] T. Wei, M. A. Carignano, I. Szleifer, Lysozyme adsorption on polyethy-
564 lene surfaces: Why are long simulations needed?, *Langmuir* 27 (2011)
565 12074–12081.
- 566 [31] T. Wei, M. A. Carignano, I. Szleifer, Molecular dynamics simulation of
567 lysozyme Adsorption/Desorption on hydrophobic surfaces, *The Journal*
568 *of Physical Chemistry B* 116 (2012) 10189–10194.
- 569 [32] J. G. Vilhena, P. Rubio-Pereda, P. Vellosillo, P. A. Serena, R. Pérez,
570 Albumin (BSA) adsorption over graphene in aqueous environment: In-
571 fluence of orientation, adsorption protocol, and solvent treatment, *Lang-*
572 *muir* 32 (2016) 1742–1755.
- 573 [33] C. Mücksch, H. M. Urbassek, Molecular dynamics simulation of free and
574 forced BSA adsorption on a hydrophobic graphite surface, *Langmuir* 27
575 (2011) 12938–12943.
- 576 [34] K. Tokarczyk, K. Kubiak-Ossowska, B. Jachimska, P. A. Mulheran, En-
577 ergy landscape of negatively charged BSA adsorbed on a negatively
578 charged silica surface, *The Journal of Physical Chemistry B* 122 (2018)
579 3744–3753.
- 580 [35] D. C. Malaspina, J. Faraudo, Molecular dynamics study of human serum
581 albumin protein corona in an inorganic nanoparticle (in preparation).
- 582 [36] L. Pérez-Fuentes, C. Drummond, J. Faraudo, D. Bastos-González, Inter-
583 action of organic ions with proteins, *Soft Matter* 13 (2017) 1120–1131.

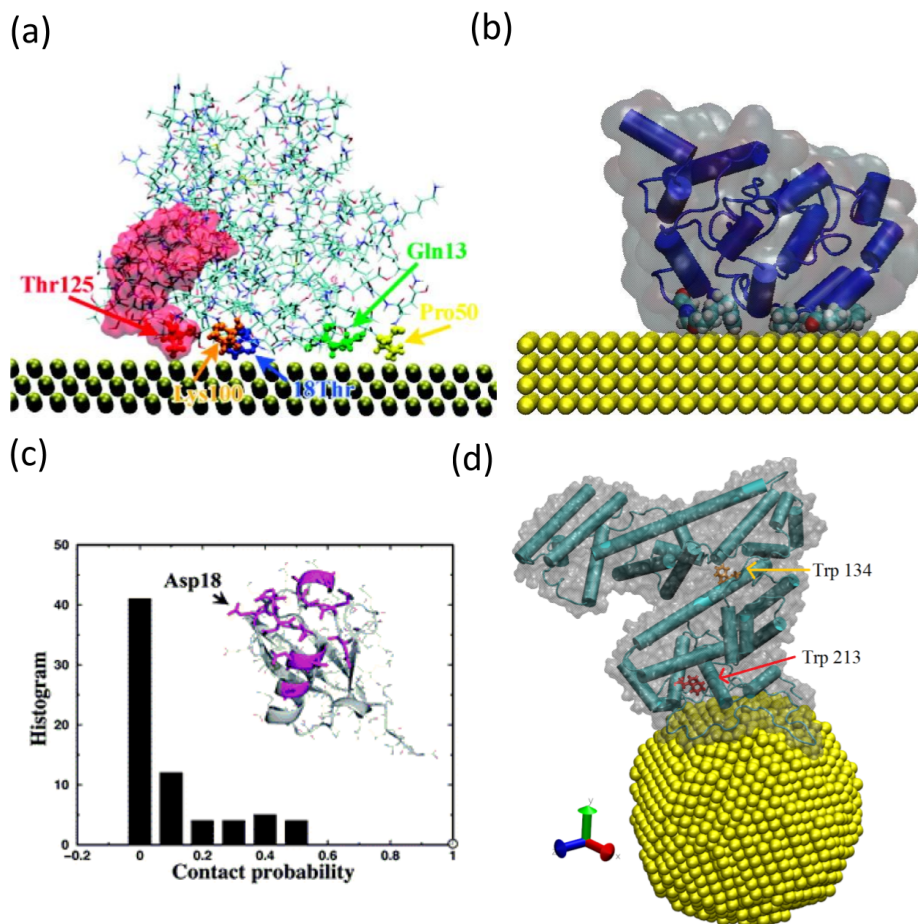


Figure 1: Examples of results from implicit solvent all-atomic MD simulations of protein adsorption (a) Adsorption of β -Lactoglobulin onto an Au(100) surface, with indication of the residues involved in protein adsorption (reproduced from [23] with permission), (b) Adsorption of β -casein onto a generic model of a planar hydrophobic surface (redrawn with data from [15]). The protein is shown in cartoon representation with indication of its size by a glassy surface. The residues involved in adsorption are shown in Van der Waals representation. (c) Simulation of adsorption of human ubiquitin over a 10nm Ag NP. The histogram indicates the number of residues with a given adsorption probability (reproduced from [14] with permission). The inset shows the structure of ubiquitin with indication of the residue with the highest adsorption probability. (d) Snapshot from a simulation of adsorption of a BSA protein over a 6nm NP, with indication of the residues with the most significant conformational change due to adsorption. Note the spread of the protein over the NP (reproduced with permission from [9]).

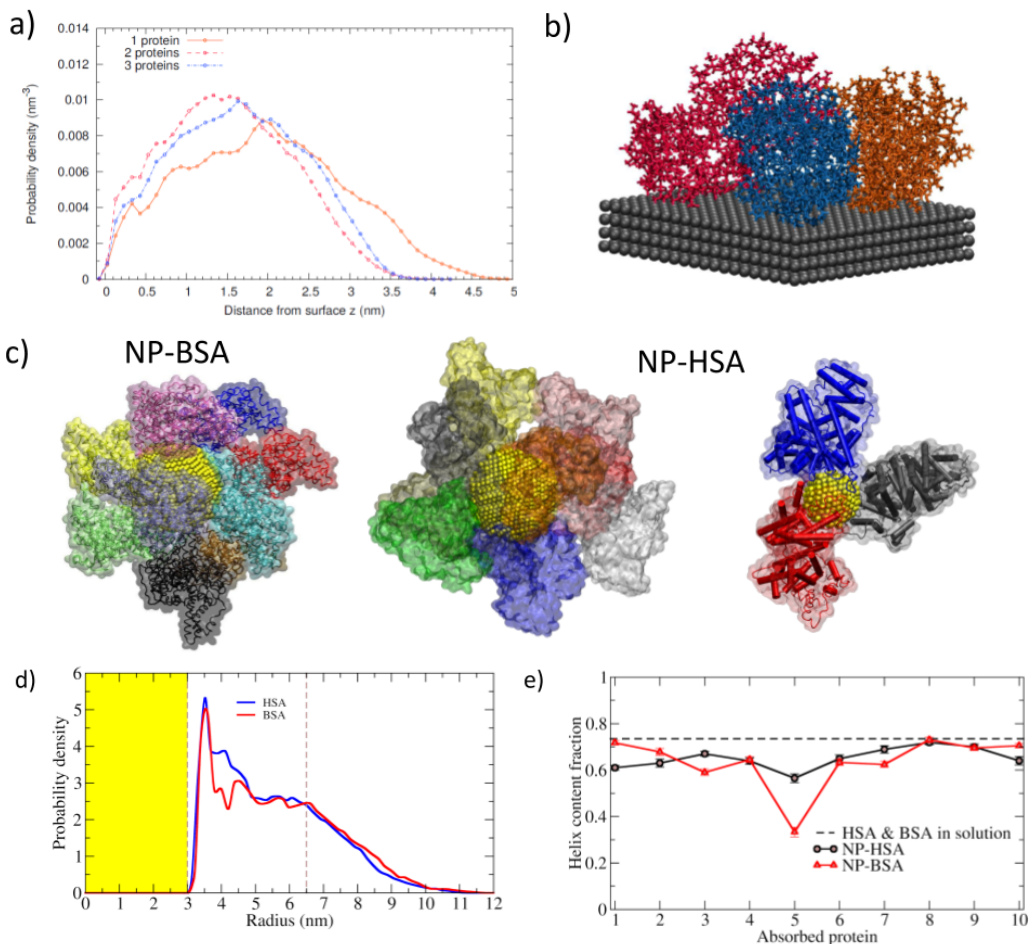


Figure 2: Examples of results from MD simulations with implicit solvent of systems with many adsorbed proteins: a) and b) correspond to a simulation of a β -casein film from [15] and (c)-(e) correspond to simulations of NP protein corona [9, 35]. (a) Probability distribution of β -casein atoms as a function of the distance from the adsorbing surface obtained in MD simulations with one, two or three proteins adsorbed onto a 45.5 nm^2 surface (b) Snapshot of the film formed by three β -casein proteins with each protein in a different colour. c) Snapshots comparing different protein corona obtained in simulations: a 6 nm NP covered with 10 BSA proteins (left), the same NP covered with 10 HSA proteins (center) and a 3 nm NP covered with HSA (right). Each colour correspond to a different protein. d) Atom density distribution (atoms/nm³) of carbon atoms from HSA or BSA proteins in the corona of a 6 nm NP. e) α -helix content for each of the 10 proteins (HSA or BSA) in the corona of a 6 nm NP compared with its value in bulk solution.